RAPID COMMUNICATIONS

PHYSICAL REVIEW B VOLUME 44, NUMBER 4 15 JULY 1991-II

Electronic states of solid C_{60}: Symmetries and photoionization cross sections

P. J. Benning, D. M. Poirier, N. Troullier, José Luís Martins, and J. H. Weaver
Department of Materials Science and Chemical Engineering, University of Minnesota, Minneapolis, Minnesota 55455

R. E. Haufler, L. P. F. Chibante, and R. E. Smalley
Rice Quantum Institute and Departments of Chemistry and Physics, Rice University, Houston, Texas 77251
(Received 19 March 1991)

Synchrotron-radiation photoemission studies of the occupied electronic states of condensed phase-pure C_{60} show sharp, well-defined features, and comparison with the calculated density of states shows excellent agreement. Studies of the emission intensities as a function of photon energy reveal remarkable modulation due to transitions to final states that retain distinct molecular character and symmetry to ~100 eV above the highest occupied level.

The discovery of an exceptionally stable structure of carbon formed by 60 atoms[1] was greeted with much interest, but the relative rarity of the molecule made extensive study of its properties difficult. With the recent breakthrough by Krätschmer *et al.*,[2] that situation has changed, and numerous experimental studies of this unique form of carbon are currently underway worldwide.

Recently, we reported a photoemission study of the electronic structure of solid C_{60} that showed 17 valence-band features.[3] Comparison of these results to calculations based on a pseudopotential plane-wave local-density-approximation formalism allowed us to identify the orbital character and symmetry of each of the valence-band features. The experimental results also demonstrated that the overall bandwidth of C_{60} was essentially the same as diamond and graphite,[4] although the sharp features of solid C_{60} were more characteristic of small molecules than solids.

This paper focuses on the variations with photon energy of the spectral features of C_{60}. We emphasize the two highest-occupied-state features because they are both p_z derived but their wave functions have opposite inversion symmetry. We show relative intensity modulation of these features with photon energies to ~100 eV, and we interpret these effects in terms of final-state symmetries and parity-selection rules. These intensity modulations provide evidence for the existence of high-lying final states that are not plane-wave-like.

C_{60} and other structures of C were formed by the contact arc method.[5] Phase-pure C_{60} was obtained by separation with toluene followed by liquid chromatography using alumina diluted with mixtures of hexanes. The resulting C_{60} was degassed at ~475 °C and then sublimed at ~550 °C. Films of solid C_{60} were grown by condensation onto freshly cleaved GaAs(110) surfaces held at ~25 °C and at pressures of $\sim 10^{-9}$ Torr. Films grown in this way have previously been imaged directly with scanning tunneling microscopy.[6] The base pressure of the spectrometer was $\sim 5\times 10^{-11}$ Torr. There was no evidence of contamination. The C_{60} layers were ~100-Å thick, as measured with a crystal-thickness monitor. The photon beam from the Aladdin light source was monochromatized and focused with the Minnesota-Argonne beamline for photon energies greater than 40 eV. A Seya-Namioka beamline was used to obtain low-energy photons. The photoelectrons were collected in an angle-integrated fashion using a double-pass cylindrical-mirror analyzer. The photon flux was determined by measuring the photocurrent from a 90% transparent tungsten mesh upstream of the sample. The total-energy resolution (electrons plus photons) was always less than 400 meV. The measurements were done at room temperature.

The upper spectrum of Fig. 1 shows a photoemission energy-distribution curve (EDC) for the leading structure

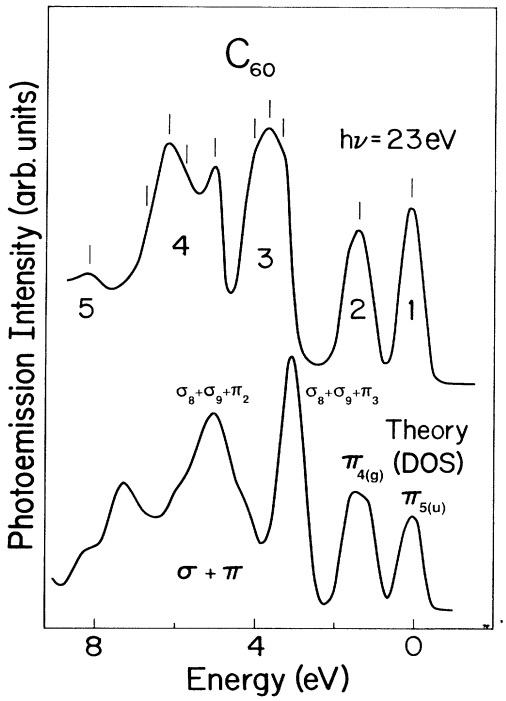

FIG. 1. High-resolution photoemission spectrum for solid C_{60} showing the initial 9 eV of the valence band where the energy is referenced to the center of feature 1. The bottom curve shows the DOS from Ref. 8 for fcc C_{60}. Features 1 and 2 are derived from π states with *ungerade* and *gerade* symmetries, respectively. Features 3–5 contain states of both σ and π character with even and odd symmetry.

of the valence band of solid C_{60}. It was obtained with $h\nu = 23$ eV and a resolution of 180 meV. The energy scale is referenced to the center of the highest-occupied-state feature which is 7.3 eV below the vacuum level.[3,7] The vertical lines identify ten spectral signatures. Feature 2 is clearly asymmetric, suggesting underlying structure, but we were unable to resolve distinct peaks for solid C_{60}. However, the gas-phase measurements of C_{60} by Lichtenberger *et al.*[7] have shown fine structure in this feature.

The lower curve of Fig. 1 shows the calculated density of states (DOS) for solid C_{60}, as discussed in Ref. 8. From the calculations, it was found that features 1 and 2 were derived almost entirely from π states with odd (*ungerade*) and even (*gerade*) symmetry, respectively.[8,9] Features 3–5 are derived from both σ and π states, and they contain states of both symmetries. The deeper valence features, not shown here, are almost entirely σ derived.[3,8,9] Comparison of the experimental and theoretical results shows very good agreement throughout the valence band, although the σ-derived states appear ~ 0.7 eV too shallow in the calculations. The greater intensity of experimental feature 1 compared to feature 2 for $h\nu = 23$ eV is a consequence of the photoionization cross section for the two initial states and is not a direct measure of the state degeneracy.

Figure 2 summarizes the variations of the C_{60} valence bands measured with photon energies of $46 \leq h\nu \leq 94$ eV in 2-eV increments. The EDCs are normalized to keep the area under feature 4 constant, and the intensities are smoothed to emphasize the major modulations as a function of photon energy. Normalization to feature 4 was done because it is derived from both σ and π states with even and odd symmetries, all in approximately equal proportions. Hence, changes in intensity for feature 4 due to variation in the symmetry and character of the photoemission final states can be expected to average out. Indeed, the integrated emission intensity of feature 4 shows only a smoothly decaying form as a function of photon energy because of the reduction in cross section and decrease in the acceptance of the electron-energy analyzer.[10] Relative intensity variations of the initial three features are easily seen over the energy range of Fig. 2. The intensity modulations of π-derived features 1 and 2 have opposite phase, indicating that the modulations reflect the character (and not merely the density) of final states. In fact, these modulations show strong symmetry dependence with intensity maxima from even initial states (feature 2) coinciding with intensity minima from odd initial states (feature 1). Feature 3 contains mixed symmetry, and its intensity modulations are more complex.

The intensity modulations of features 1 and 2 can be explained by initial- and final-state symmetry and parity selection rules. The operator responsible for photoemission, namely $\mathbf{A}\cdot\mathbf{p}$ in the dipole approximation, is odd under reflection. To conserve parity, an electron can only be excited from even to odd or from odd to even states by the dipole operator, i.e., it must change parity upon photoexcitation. This parity selection rule implies that emission from even initial states will be enhanced and emission from odd initial states will be reduced by excitation into a region of final states with predominantly odd symmetry. Thus, changes in cross section for initial states with opposite symmetry, such as the first two valence features of C_{60}, can be used to examine the symmetry of the empty states.

Figure 3 shows the variations in intensity of features 1 and 2 for final-state energies ~ 10–120 eV above the highest occupied level. These intensities are normalized to the intensity of feature 4, as in Fig. 2, and plotted as I_1/I_4 and I_2/I_4 in the top panel of Fig. 3. Each maximum from an odd state (feature 1,π_μ) is matched by a minimum in intensity from an even state (feature 2,π_g). This behavior seems to indicate that there are large variations in the

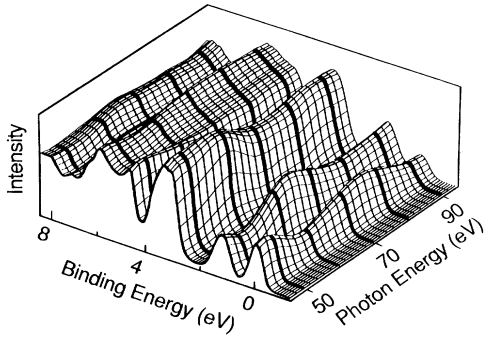

FIG. 2. Intensity variations of valence-band EDCs for C_{60} as a function of photon energy. Features 1 and 2 identified in Fig. 1 exhibit intensity modulations related to their opposite symmetry and parity selection rules. Features 3–5 are of mixed character and symmetry.

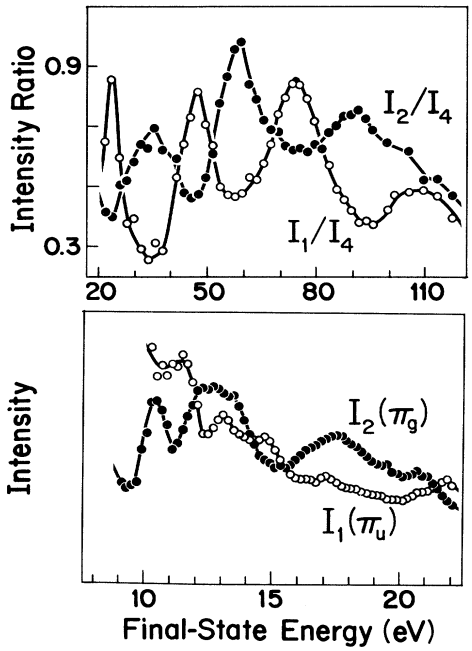

FIG. 3. Intensity variations of features 1 and 2 as a function of final-state energy relative to the center of feature 1. The top panel shows intensities normalized to feature 4 while the bottom panel shows absolute intensity variations at lower final-state energy.

DOS for empty odd and even states up to 120 eV, although the total DOS is probably relatively featureless. The lower panel of Fig. 3 shows corresponding variations of I_1 and I_2 in the range 10–23 eV where normalization to I_4 is impossible. Again, modulations can be attributed to changes in the symmetry of the final states. Indeed, no other explanation can account for the clear symmetry dependence and nonperiodicity in energy, momentum, or wavelength.[11]

The experiments suggest that the density of states of C_{60} with a given symmetry retains structure for final-state energies of 100 eV above the highest occupied levels. This would not occur if the final states were essentially plane-wave-like. Although reliable C_{60} wave functions could not be calculated for these high energies because of the large number of electrons per unit cell, calculations could be done to examine the character of the corresponding states in graphite. In that case, we found that the density of states has noticeable deviations from a square-root behavior up to ~70 eV and that non-plane-wave-like states are present above 100 eV. In fact, Bianconi, Hagström, and Bachrach[12] reported intensity variations for graphite that persisted up to 90 eV. In that work, two valence-band initial states with inequivalent character were selected and intensities of those features were measured as a function of photon energy. A plot of graphite of the intensity ratio of π-derived to σ-derived initial states as a function of final-state energy shows modulations of similar width but with much less magnitude than those of Figs. 2 and 3 for C_{60}. While their presence supports our analysis, the degree to which the intensities change in C_{60} indicates more pronounced final-state effects in the molecular solid than in the layered material.

Figure 4 focuses on the $h\nu$ variation of feature 4 for $18.8 \leq h\nu \leq 21.4$ eV. As can be seen, the intensity of the peak at 6.3 eV is relatively weak at $h\nu = 18.8$ eV but is very strong at $h\nu = 21.4$ eV. Calculations of the distribution of occupied states show that the 6.3-eV peak is derived from a group of 12 states with symmetries h_g, g_g, and t_g. Analysis of their wave functions shows that they correspond to σ_8 states, i.e., states that form σ bonds between carbon atoms and that have an angular decomposition with respect to the center of the molecule dominated by an $l = 8$ component, as discussed in Ref. 8. Large oscillator strengths are expected for excitation from these levels into σ_0 orbitals, which the calculations predict[8] could be accessed with photons of energy ~13 eV but which lie below the vacuum level. Weaker transition probabilities are then predicted until $h\nu \sim 20$ eV because of the l character of the final states. In the region corresponding to $h\nu \sim 20$ eV, the calculations predict two types of empty states, namely nonmolecular, delocalized levels and antibonding σ states. Among them are σ_{11} levels that exhibit significant mixing with σ_9 states. Significant transition probabilities are again expected to these final states. Hence, we tentatively associate the suppression of the 6.3-eV peak to unfavorable matrix elements for $h\nu \sim 18$ eV.

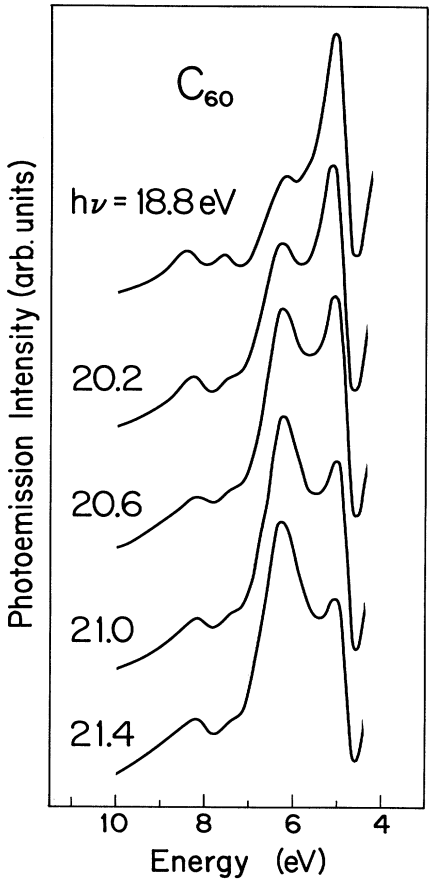

FIG. 4. Line-shape changes for feature 4 as a function of photon energy showing suppression of the 6.3-eV features for $h\nu \sim 18$ eV. Calculations suggest that the initial-state feature at 6.3 eV is σ_8 derived and that there is an absence of suitable final states until $h\nu \sim 20$ eV when empty σ_{11} levels become accessible.

The valence-band features of C_{60} exhibit a greater variation in intensity as a function of photon energy than the corresponding features of any other molecule or solid structure to date. These variations reflect the unique structure of C_{60} and the retention of molecular symmetry far into the empty-state regions.

This work was supported by the National Science Foundation, the Office of Naval Research, and the Robert A. Welch Foundation. The calculations were supported by the Minnesota Supercomputer Institute. The synchrotron-radiation photoemission studies were performed at Aladdin, a user facility supported by the National Science Foundation, and the assistance of its staff is gratefully acknowledged.

[1]H. W. Kroto, J. R. Heath, S. C. O'Brian, R. F. Curl, and R. E. Smalley, Nature (London) **318**, 162 (1985).

[2]W. Krätschmer, L. D. Lamb, K. Fostiropoulos, and D. R. Huffman, Nature (London) **347**, 354 (1990).

[3]J. H. Weaver, José Luís Martins, T. Komeda, Y. Chen, T. R. Ohno, G. H. Kroll, N. Troullier, R. E. Haufler, and R. E. Smalley, Phys. Rev. Lett. **66**, 1741 (1991).

[4]F. R. McFeely, S. P. Kowalczyk, L. Ley, R. G. Cavell, R. A. Pollak, and D. A. Shirley, Phys. Rev. B **9**, 5268 (1974).

[5]R. E. Haufler *et al.*, J. Phys. Chem. **94**, 8634 (1990); R. E. Haufler, Y. Chai, L. P. F. Chibante, J. Conceicao, C.-M. Jin, L.-S. Wang, S. Maruyama, and R. E. Smalley, in *Clusters and Cluster-Assembled Materials,* edited by R. S. Averback, D. L. Nelson, and J. Bernholc, MRS Symposia Proceedings No. 206 (Materials Research Society, Pittsburgh, 1991).

[6]Y.Z. Li, J. C. Patrin, M. Chander, J. H. Weaver, L. P. F. Chibante, and R. E. Smalley, Science **252**, 547 (1991).

[7]D. L. Lichtenberger, M. E. Jatcko, K. W. Nebesny, C. D. Ray, D. R. Huffman, and L. D. Lamb, in *Clusters and Cluster-Assembled Materials* (Ref. 5); D. L. Lichtenberger, K. W. Nebesny, C. D. Ray, D. R. Huffman, and L. D. Lamb, Chem. Phys. Lett. **176**, 203 (1991).

[8]J. L. Martins, N. Troullier, and J. H. Weaver, Chem. Phys. Lett. (to be published).

[9]See the calculations by S. Satpathy, Chem. Phys. Lett. **130**, 545 (1986); R. L. Disch and J. M. Schulman, Chem. Phys. Lett. **125**, 465 (1986); H. P. Lüth and J. Almlöf, Chem. Phys. Lett. **135**, 357 (1987); P. D. Hale, J. Am. Chem. Soc. **108**, 6087 (1986); S. Larsson, A. Volosov, and A. Rosén, Chem. Phys. Lett. **137**, 501 (1987); A. Rosén and B. Wästberg, J. Chem. Phys. **90**, 2525 (1989); Q. Zhang, Yae-Yel Yi, and J. Bernholc, Phys. Rev. Lett. **66**, 2633 (1991); S. Saito and A. Oshiyana, *ibid.* **66**, 2637 (1991); J. W. Mintmire, B. I. Dunlap, D. W. Brenner, R. C. Mowrey, and C. T. White, Phys. Rev. B (to be published).

[10]P. W. Palmberg, J. Electron Spectrosc. Relat. Phenom. **5**, 691 (1974).

[11]Diffraction effects can modulate photoemission cross sections, but they would not produce symmetry-dependent modulations and they would be periodic.

[12]A. Bianconi, S. B. M. Hagström, and R. Z. Bachrach, Phys. Rev. B **16**, 5543 (1977).